Surface area of carbon-based nanoparticles prevails on dispersion for growth inhibition in amphibians

Laura Lagier, Florence Mouchet, Christophe Laplanche, Antoine Mottier, Stéphanie Cadarsi, Lauris Evariste, Cyril Sarrieu, Pierre Lonchambon, Eric Pinelli, Emmanuel Flahaut, et al.

Surface area of carbon-based nanoparticles prevails on dispersion for growth inhibition in amphibians

L. Lagier [a], F. Mouchet [a, *], C. Laplanche [a], A. Mottier [a], S. Cadarsi [a], L. Evariste [a], C. Sarrieu [b, c], P. Lonchambon [b, c], E. Pinelli [a], E. Flahaut [b, c], L. Gauthier [a]

[a] *EcoLab, Université de Toulouse, CNRS, INPT, UPS, Toulouse, France*
[b] *Université de Toulouse, INP, UPS, Institut Carnot CIRIMAT (Centre Inter-universitaire de Recherche et d'Ingénierie des Matériaux), UMR CNRS 5085, F-31062, Toulouse Cedex 9, France*
[c] *CNRS, Institut Carnot CIRIMAT, F-31062, Toulouse, France*

A B S T R A C T

The attractive properties of carbon-based nanoparticles such as graphene and its derivatives or carbon nanotubes lead to their use in many application fields, whether they are raw or functionalized, such as oxidized. These particles may finally contaminate the aquatic compartment, which is a major receptacle of pollutants. The study of their impact on aquatic organisms is thus essential. At the nano scale, recent studies have highlighted that specific surface area should be used as the most relevant descriptor of toxicity instead of the conventional mass concentration. By using a dose-response model, this work compares the chronic toxicity observed on *Xenopus laevis* larvae after 12-day *in vivo* exposure to raw, oxidized carbon allotropes, or in the presence of chemical dispersant. We show that chemical dispersion does not influence the observed chronic toxicity, whether it is through surface chemistry (oxidation state) or through the addition of a dispersant. The biological hypothesis leading to growth inhibition are discussed. Finally, these results confirm that surface area is the more suited metric unit describing growth inhibition.

1. Introduction

Carbon-based nanoparticles (CNPs) such as graphene related materials (GRMs), carbon nanotubes (CNTs) and nanodiamonds (NDs) have outstanding properties making them attractive in an increasing number of applications [1–6]. Such properties are made possible by the nanometric scale of CNPs which allows them to behave differently from bulk materials of the same element. Each CNP is defined by its own unique characteristics including especially its specific surface area (SSA). It is known that the ratio between the number of atoms at the surface and in the bulk increases exponentially with decreasing particle size, making the surface reactivity more and more important [7,8]. This supposes that for a given mass, a CNP with a larger surface area should be more biologically reactive than a CNP with a smaller one. As non-soluble materials, the biological reactivity would be the interaction between the atoms located at the surface of the CNPs with the biological target. Thus, toxicity studies [7,9,10] which generally deal with aerial toxicity argue that the conventional expression of the concentration in terms of mass should be discouraged to predict the biological effects of CNPs in favor of surface area (in $m^2\ L^{-1}$) which would be a more relevant dose metric describing these effects whatever the structure of the CNPs.

Our recent ecotoxicological study in amphibians [11] leads to the same conclusion: the effect of several allotropes of carbon on *Xenopus laevis* growth rate was investigated and the results clearly showed that surface area is the best descriptor of toxicity at high doses. However, only raw nanoparticles were considered in this previous work, whereas numerous commercial CNPs are most often functionalized (either covalently by oxidation, or non-covalently by addition of dispersants). Moreover, if they are released into the environment, CNPs could interact with natural organic matter and/or different chemical adsorbents, which can affect their dispersion state [12]. Most of *in vivo* studies generally report higher toxicity induced by such dispersed CNPs [13–17]. On the contrary, depending on the tested organism, others report a mitigate toxicity by testing such CNPs, like Li et al. [18] who suggest

* Corresponding author.
E-mail address: florence.mouchet@ensat.fr (F. Mouchet).

http://dx.doi.org/10.1016/j.carbon.2017.04.016

that organic matter coated on fullerene crystals could hinder their direct contact with cells.

To our knowledge, this study is the first to investigate if CNPs toxicity in water is defined by their surface chemistry (bare carbon atoms, oxygen groups, or adsorbed organic compounds) or only by their surface area itself. Modifying surface chemistry of CNPs is likely to influence their state of dispersion in the aqueous medium. The present work aims at investigating how different routes of dispersion in water: covalent (grafting of oxygen-containing functions) or non-covalent (adsorption of a chemical dispersant) may impact the potential chronic toxicity in amphibians. As an extension of our first study on the subject [11], this work also focuses on the same model organism, *Xenopus laevis*, as a well-known ecotoxicological model, especially for the evaluation of the CNPs toxicity [19,20]. Its physiology makes it particularly sensitive to the presence of contaminants in water [21], so that it is more and more used as monitoring system for water quality assessment [22]. Growth rate was investigated in larvae as a sensitive response that expresses the global health status of the living organisms. To keep continuity, the results concerning raw CNPs of our previous study [11] (double and multi-walled CNTs: DWCNTs and MWCNTs; few layer graphene: FLG; nanodiamonds: NDs) are reminded in this paper in order to provide an easier comparison between raw and dispersed counterparts. Covalent dispersion was investigated by exposing *Xenopus laevis* larvae to oxidized CNPs, namely oxidized DWCNTs (DW-ox) and graphene oxides (GO-A and GO-B), while in order to tackle more environmentally realistic conditions, non-covalent dispersion was tested *via* DWCNTs in the presence of commercial Suwannee River natural organic matter (SRNOM), and MWCNTs in the presence of carboxymethyl cellulose (CMC). This work is focusing on stable and non-soluble carbon nanoparticles in environmental conditions, thus excluding for example small-size fullerenes which are molecules and spontaneously oxidize in water to form soluble fullerol derivatives.

2. Experimental

2.1. Synthesis and characterization of the studied CNPs

DWCNTs were synthetized by catalytic chemical vapor deposition (CCVD) as already described by Flahaut et al. [23]. MWCNTs (Graphistrength batch 09215) were provided by Arkema France and described by Bourdiol et al. [24]. Oxidized DWCNTs (DW-ox) were prepared by oxidation of the initial raw DWCNTs by a treatment with 3 M HNO_3 at 130 °C (24 h) in reflux conditions. DW-ox were washed with deionized water by filtration on polypropylene membrane (0.45 μm pore size). Finally, DW-ox were freeze dried. GOs (batch A (xGO- 116) and B (nxGOH_37B), respectively GO-A and GO-B) were provided by Antolin Group and prepared by oxidation of GANF© (Grupo Antolin Carbon Nanofibers) using the Hummer's method [25,26].

Physico-chemical characteristics of the tested CNPs are detailed in Table 1. Elemental analysis was performed by CHNS organic elementary analysis. Specific surface area was measured using the Brunauer, Emett and Teller's method (BET) (N_2 adsorption) on powdered samples of CNPs.

Fig. 1 shows the difference of morphology between the tested CNPs. Compared to their raw counterparts [19,24,29], particles presented here appear less agglomerated and better dispersed.

2.2. Chemical dispersants

Commercial Suwannee River natural organic matter (SRNOM; Cat no. 1R101N) was purchased from the International Humic Substances Society (IHSS, St Paul, MN, USA) and was added to each DWCNT suspension at a 1:1 ratio. This ratio was found sufficient to stabilize the dispersion of each DWCNT concentration. SRNOM is a natural mixture of humic substances, initially provided at 8.5% (w/w) of humidity, with a high content in organic matter, and a low amount of salts as described in Verneuil et al. [30,31]. Elemental analysis gives a composition of 52.47% of carbon, 42.69% of oxygen, 4.19% of hydrogen, 1.1% of nitrogen, 0.65% of sulfur and 0.02% of phosphorus (w/w).

Carboxymethyl cellulose (CMC) ($C_{28}H_{30}Na_8O_{27}$, Fluka) is a water-soluble, anionic polymer which is massively used in food industry as additive (E466), and also in cosmetics and pharmaceuticals, as described in Bourdiol et al. [24]. Here, each suspension of MWCNTs was prepared with addition of CMC at 50 $mg.L^{-1}$, because the effectiveness of dispersion by using CMC was found optimal at this concentration [24].

Both SRNOM and CMC are found non-toxic towards *Xenopus* larvae.

2.3. CNP physical dispersion and contamination of the exposure media

The desired amount of CNP powder was first weighed and dispersed in deionized water (together with a chemical dispersant or not) to obtain a stock suspension. The latter was homogenized (except for GOs which is already rather hydrophilic, and in order not to decrease its size) by physical dispersion using appropriate mechanical methods such as shear mixing with a homogenizer (SILVERSON L5M) at 8000 rpm followed by a pulsed sonication of 30 min (Vibra-cell 75042 -500 W – 3s on/3s off) with a probe of 1 cm diameter at 30% amplitude.

Then, depending on the target concentration, required amounts of this stock suspension were sampled under ultrasonic bath before being introduced in individual glass test tubes and adjusted to 20 mL by addition of deionized water. For each concentration, 12 test tubes of 20 mL were thus prepared, corresponding to the number of exposure days.

Afterwards, just prior to contamination of the water column, the 20 mL suspensions of CNPs were dispersed 2 min in an ultrasonic bath (Bioblock 89863, typ 570 HF Freq 35 kHz). Finally, they were poured in crystallizing dishes and the test tubes were rinsed twice with reconstituted water (RW) to collect remaining CNPs on the tubes walls. Crystallizing dishes were finally leveled to 2L with RW before introducing the organisms.

2.4. Xenopus rearing and breeding

Spawning of *Xenopus* was induced by injection of 50 IU of pregnant mare's serum gonadotropin (PMSG 500; Intervet, France, [9002-70-4]) in males and of 750 IU of human chorionic gonadotropin (HCG; Organon, France, [9002-61-3]) in females. Viable eggs were bred at 22 ± 2 °C in normal tap water filtered through active charcoal. As soon they got self-feeder, larvae were fed with dehydrated aquarium fish food (Tetraphyll®). They could both feed directly in the water column where they lived, as they are filter-feeders, but they also mainly grazed settled food at the bottom of the containers. Larvae were bred in this way until they reached an adequate development stage for experimentations.

2.5. Exposure conditions

Xenopus larvae at stage 50 according to the development table of Nieuwkoop & Faber [32] were exposed 12 days in semi-static conditions based on the international standard 21427-1 [33]. The animals were submitted to a natural light-dark cycle at 22 ± 0.5 °C and fed every day with fish food TetraPhyll®. Water used for the

Table 1
Physico-chemical characteristics of the carbon-based nanoparticles. SWCNTs: single-walled CNTs; TWCNTs: triple-walled CNTs; wt.%: weight %; NA: not available.

	DW-ox	DW-SRNOM	MW-CMC	GO-A	GO-B
Synthesis/production	HNO_3 3 M at 130 °C during 24 h of raw DWCNTs	Catalytic chemical vapor deposition		GANF© processed by Hummer's method	
Catalyst in starting material	Co/Mo-MgO	Co/Mo-MgO	Fe-Al_2O_3	Ni, Fe, Co	
Carbon content	88.3 wt%	92.0 wt%	~92.0 wt%	45.2 wt%	48.0 wt%
Oxygen content	11.7 wt%	3.5 wt%	~1 wt%	51.3 wt%	48.2 wt%
Number of walls/layers (HRTEM)	80% DWCNTs, 15% SWCNTs, 5% TWCNTs	80% DWCNTs, 15% SWCNTs, 5% TWCNTs	5-15 (100% MWCNTs)	1-5 [27,28]	
Size (TEM)	1 to 100 μm length, 1–3 nm ø	1 to 100 μm length, 1–3 nm ø	0.1–10 μm length, 10–15 nm ø	0.2–8 μm	0.2–8 μm
Specific surface area (BET)	300 $m^2\ g^{-1}$	980 $m^2\ g^{-1}$	235 $m^2\ g^{-1}$	228 $m^2\ g^{-1}$	206 $m^2\ g^{-1}$

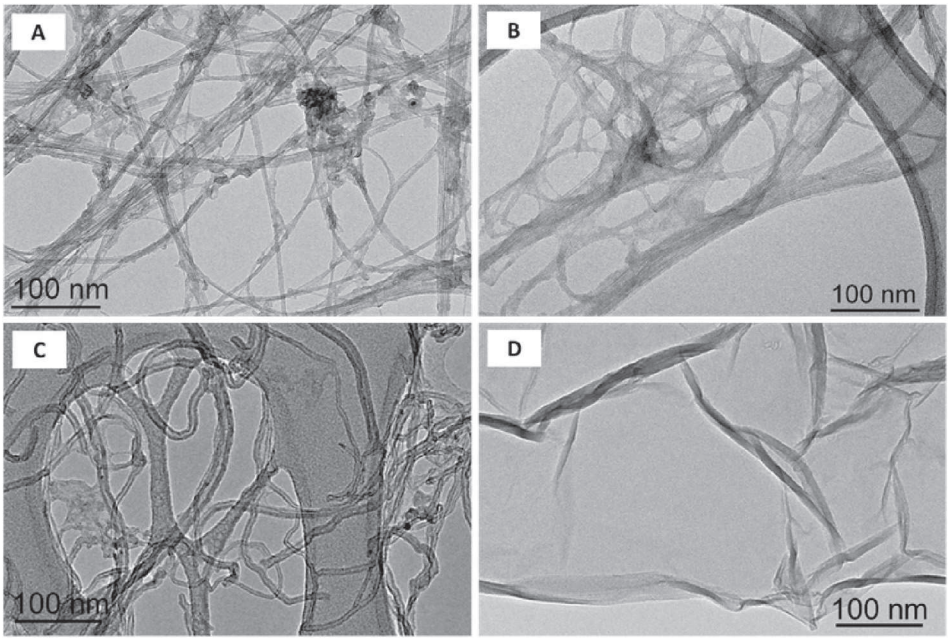

Fig. 1. Transmission electron microscopy micrographs of (A) DW-ox, (B) DW-SRNOM, (C) MW-CMC, (D) GO-A. GO-B is not shown here but is similar to GO-A.

experiment was reconstituted from distilled water added with nutritive salts: 294 mg L^{-1} $CaCl_2{\cdot}2H_2O$; 123.25 mg L^{-1} $MgSO_4{\cdot}7H_2O$; 64.75 mg L^{-1} $NaHCO_3$; 5.75 mg L^{-1} KCl. A concentration range from 0.05 to 50 mg L^{-1} of oxidized CNPs and raw CNPs in the presence of a dispersant was tested on *Xenopus*: DW-ox, GO-A, GO-B, DWCNTs with the addition of SRNOM (DW-SRNOM) and MWCNTs with the addition of CMC (MW-CMC). Larvae were grouped in batches of 20 animals in crystallizing dishes and exposed to CNPs in RW or in negative control (NC) media (RW alone). *Xenopus* were also exposed in RW to SRNOM and CMC alone (without CNPs). Whatever the condition, pH of the media was about 7 ± 1 in compliance with the international standard 21427-1 [33].

After 12 days of exposure, the size of larvae was measured. Larvae were dissected under binocular and macro observations of the intestines and the gills were performed.

2.6. Chronic toxicity and calculation models

The size of each larvae was measured at the beginning (d_0) and at the end (d_{12}) of the exposure using the ImageJ 1.49 software. In order to be compared, sizes were then normalized as described in our previous study [11] according to the following formula:

$$Normalized\ size\ (\%) = \left(\frac{Ld_{12} - MLd_0}{MLd_0} \times 100\right) \times \left(\frac{100}{MLCd_{12}}\right)$$

Ld_{12} is the length of one individual larva at 12 days, MLd_0 is the mean length of the group of the exposed larvae at day 0, and $MLCd_{12}$ is the mean length of the NC group at day 12.

Then, in order to express normalized size as a function of mass or surface concentration, the corresponding metrics for each dose to which larvae were exposed (Table 2) were investigated. Surface concentrations ($m^2\ L^{-1}$) were calculated as follows:

$$Surface\ concentration = \frac{SSA \times M}{1000}$$

Where *SSA* is the specific surface area ($m^2.\ g^{-1}$) of a given CNP (see Table 1 for SSA values) and *M* is the mass (mg) of CNP used per liter of RW.

Thus, amphibian dose-response growth inhibition could be modeled by predicting the normalized size using the following two-parameter logistic equation as previously detailed [11]:

Table 2
Corresponding metrics for each dose (A-F) of carbon-based nanoparticles (CNPs) to which *X. laevis* larvae were exposed. NT: no tested.

CNPs	Mass concentration ($mg.L^{-1}$)						Surface concentration ($m^2.L^{-1}$)					
	A	B	C	D	E	F	A	B	C	D	E	F
GO-A	NT	0.10	NT	1	10	50	NT	0.02	NT	0.23	2.28	11.4
GO-B	0.05	0.10	0.15	1	10	NT	0.01	0.02	0.03	0.21	2.06	NT
DW-ox	NT	0.10	NT	1	10	50	NT	0.03	NT	0.3	3	15
DW-SRNOM	NT	0.10	NT	1	10	NT	NT	0.10	NT	0.98	9.8	NT
MW-CMC	NT	0.10	NT	1	10	50	NT	0.02	NT	0.24	2.35	11.75

$$E\left(Normalized\ size_{ijk}\right) = \frac{100}{1 + \left(\frac{x_{ijk}}{EC_{50,\ i}}\right)^{1/\alpha_i}}$$

where x_{ijk} is the dose and i, j, and k are the indices over dose metrics, CNPs, and concentrations, respectively. $EC_{50,i}$ is the value of dose metric i when the predicted size reaches 50%. At this point, the slope is $-25/EC_{50,i}\alpha_i$.

Sizes were measured with errors of different magnitudes (heteroscedasticity). Consequently, the data had to be fitted using nonlinear weighted least-squares regression. In order to find which dose metric is the best descriptor of growth rate, two models were compared, each using one of the dose metric as a predictor, and their performances were evaluated *via* their R^2 and Akaike information criterion (AIC). R^2 measures the proportion of the variance of the response variable which is "explained" by the model (higher R^2 are deemed better). R^2 values are easy to compute and are comparable between models and between studies even by using distinct datasets. R^2 as such, however, does not take into consideration heteroscedasticity, nor differences of model complexities, and the level of significance of R^2 differences is left to the user's opinion, which use is consequently limited in model selection [34]. AIC, on the other hand, is a trade-off between goodness-of-fit and complexity (lower AIC are deemed better) and fully takes into consideration measurement errors. Only the difference between two AIC values (AIC_A and AIC_B; $AIC_A > AIC_B$) which originates from two models (models A and B) which simulate the same response variable with the same data is relevant, and in that case the evidence ratio exp (AIC_A-AIC_B/2) indicates how much more likely model A is than model B [35]. Statistical computations were carried out with R 3.1.3 [36].

Finally, statistical differences of normalized growth rate between *X. laevis* larvae exposed to each dose of CNPs (from A to F) and the NC group were performed using Student's t-test. Normality requirement and homoscedasticity were fulfilled according to Shapiro-Wilk test and Fisher's test, respectively. Results are shown in Table 3.

3. Results

3.1. Chronic toxicity

No significant growth inhibition was observed in larvae exposed to CMC and SRNOM alone. Size of larvae exposed to CNPs decreased with increasing concentrations. A significant growth inhibition was observed in larvae exposed to GO-B, DW-SRNOM and MW-CMC from concentration E, and exposed to GO-A and DW-ox at the concentration F (Table 3).

Normalized size was plotted as a function of mass (Fig. 2 A) and surface area of CNPs (Fig. 2 B). The model using surface area presents an AIC of 3031.3, against 3009 for the model involving mass concentration, which corresponds to an important difference in spite of the order of magnitude of the values [35]. This statistical discard between these two AIC values represents the probability that the mass model is 69564 less probable than the surface area model. In the same way, goodness of fit was found better for the model using surface area ($R^2 = 0.87$) than for the model using mass concentration ($R^2 = 0.73$), indicating that surface area described better larvae growth than mass.

3.2. Macro-observations of dissected larvae

As evidenced in earlier studies on raw CNPs [19,20,37], the dissections revealed the presence of dark agglomerates in the digestive tract and in gills of larvae exposed to each CNP compared to the NC larvae (Fig. 3). These black masses correspond to CNP agglomerates and were more and more visible in the gut as the exposure concentration increased, whatever the tested nanoparticle. The same dose-dependent observations were made on the gills of the exposed larvae.

4. Discussion

The aim of this study is to assess the influence of carbon-based nanoparticles on growth inhibition of the model organism *Xenopus laevis*, a filter-feeder amphibian larva, combined with an original approach to determine the dose-response relation based on surface area, as the most relevant descriptor [11]. In the present study, a particular interest was assigned to analyze the effect of the dispersion state of different CNPs on larvae growth, dispersed or not by organic matter (non-covalent dispersion), or functionalized by oxidation (covalent dispersion) in order to obtain a good dispersion without any additive.

4.1. Metric doses

Data show that CNPs induce a dose-dependent growth inhibition after 12 days of exposure (Table 3). On the basis of the classical

Table 3
Growth in *X. laevis* larvae exposed to each dose (A-F) of carbon-based nanoparticles. Results are given as the normalized mean (%) ± Standard Error of the Mean (SEM). "*" significantly different size of larvae compared to the NC group for $p \leq 0.05$; "**" significantly different size of larvae compared to the NC group for $p \leq 0.01$; "***" significantly different size of larvae compared to the NC group for $p \leq 0.001$; NC: negative control; NT: no tested.

	NC	A	B	C	D	E	F
GO-A	100.00 ± 3.23	NT	100.20 ± 2.98	NT	100.29 ± 2.58	90.71 ± 2.6*	50.36 ± 3.16***
GO-B	100.00 ± 3.59	99.82 ± 5.37	97.52 ± 4.77	101.23 ± 3.87	97.46 ± 2.69	72.49 ± 4.48***	NT
DW-ox	100.00 ± 4.48	NT	106.27 ± 2.69	NT	95.67 ± 2.78	91.12 ± 2.62	49.08 ± 2.61***
DW-SRNOM	100.00 ± 3.62	NT	108.80 ± 3.88	NT	96.51 ± 2.45	61.35 ± 2.97***	NT
MW-CMC	100.00 ± 1.26	NT	94.24 ± 1.26**	NT	96.97 ± 1.63	86.12 ± 2.43***	31.66 ± 2.96***

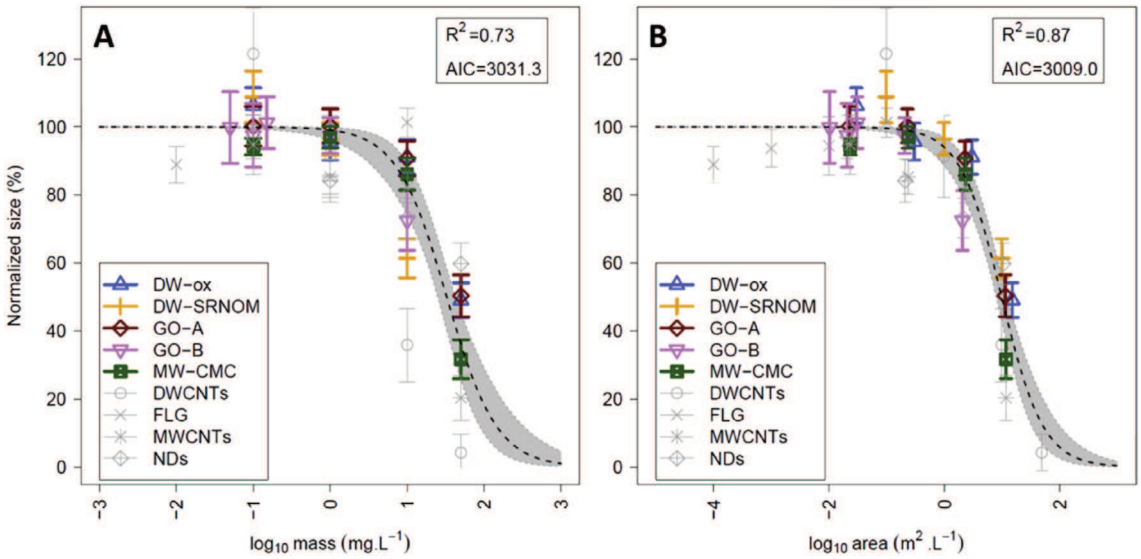

Fig. 2. Growth inhibition in *X. laevis* larvae after 12 days of exposure to DW-ox, GO-A, GO-B, DW-SRNOM and MW-CMC. Raw CNPs (few layer graphene, FLG; nanodiamonds, NDs; DWCNTs; MWCNTs) from previous study [11] are reminded in grey. Normalized size (%) is plotted *vs* the base-10 logarithms of two different metrics: mass concentration (mg.L^{-1}) (2.A) and surface area concentration (m^2 L^{-1}) (2.B). Black dashed lines represent nonlinear regression model predictions, and shaded areas are 95% confidence intervals (CIs) on these. The 95% CIs on the mean sizes, which were computed from the experimental assays, are represented as vertical error bars. (A colour version of this figure can be viewed online.)

mass concentration unit, GO-A could be considered as the least toxic CNP since it induces the lowest growth inhibition. Thus, the ascendant toxicity level of CNPs (including raw CNPs described by Mottier et al. [11]) could be ordered as follows: FLG (few layer graphene) > GO-A > DW-ox > NDs (nanodiamonds) > MW-CMC > GO-B > MWCNTs > DW-SRNOM > DWCNTs.

However, as CNPs behave differently from classical chemicals because of their physico-chemical characteristics, the classical approach based on mass concentration could lead to mis-interpretations. Thus, some authors proposed to use the surface area unit as a better descriptor of the CNP biological effects [7,9–11] than mass concentration. In order to determine if this new approach was relevant to describe the growth inhibition induced by the tested CNPs, in our experimental conditions, normalized sizes of larvae were plotted as a function of the two units. Fig. 2 shows a comparison between growth inhibition of *Xenopus laevis* larvae expressed *vs* mass concentration (Fig. 2 A) or surface area concentration (Fig. 2 B).

The quality of models involving the two dose metrics was compared using the AIC values (Fig. 2). This statistical discard between these two AIC values represents the probability that the mass model is 69564 less probable than the surface area model. This statistical approach demonstrates that growth inhibition mechanisms were most dependent on the surface area of the CNPs than on their mass.

In the same way, goodness of fit was found better for the model using surface area than for the model using mass concentration (Fig. 2). In compliance with the corresponding coefficient of determination of our previous work (R^2 = 0.88 for the surface model) [11], our value (R^2 = 0.87) demonstrates the good ability of the logistic equation to describe the process generating the data. The similarity between the R^2 values related to surface model from our first study based on raw CNPs only [11] and our present results relative to dispersed CNPs suggests that CNP surface area is adequate to predict *Xenopus* growth rate in both cases, irrespectively of CNP allotropic form (1D for nanotubes and 2D for graphenes) or their state of dispersion and oxidation level. Moreover, the global surface concentration for which 50% of growth inhibition was observed (EC_{50}) was estimated to be 9.85 m^2. L^{-1}. This value is in agreement with our previous work where EC_{50} was found just slightly lower (7.47 m^2. L^{-1}) [11]. These results confirm that CNPs are responsible for growth inhibition mechanisms related to their surface area, regardless of their other physico-chemical properties. To give a correspondence with an EC_{50} based on mass concentration, this would correspond to values from 10 mg L^{-1} for DWCNTs/DW-SRNOM (which have a high SSA) to 985 mg L^{-1} for the raw FLG described previously [11] (which has a low SSA).

4.2. State of dispersion

In the present study, the results of the model demonstrate that larvae growth appeared to be ruled by CNP surface area, as if their state of dispersion could be neglected. This conclusion contrasts with the literature which generally reports, on the basis of mass concentration and depending on organisms and exposure circumstances, higher [16,17,38] or lower [18] toxic effects for dispersed CNPs compared to their raw counterparts.

In this work, two allotropic forms of carbon and two modes of dispersion are used: non-covalent dispersion with natural organic matter or carboxymethyl cellulose, and covalent dispersion by functionalization (oxidation). Note that other parameters that could influence the stability of CNP dispersions (pH and salt concentration of the medium [39]) were constant. Whatever the mode of dispersion used, functionalized (covalently or not) CNPs are better dispersed in water than raw CNPs [40,41]. Indeed, carbon surfaces tend to be attracted by each other because of van der Waal's forces [42]. In absence of organic matter, raw CNPs tends to rapidly agglomerate and settle down. The example of raw MWCNT dispersion observed in Fig. 4 A highlights this heterogeneous aspect of the dispersion at the beginning of each medium renewal (every 24 h).

In the presence of organic matter (SRNOM or CMC), CNPs form non-covalent bonds with the dispersant which allow to maintain their individual dispersion in the water column [43]. The fulvic and humic acids of the natural organic matter could thus be adsorbed

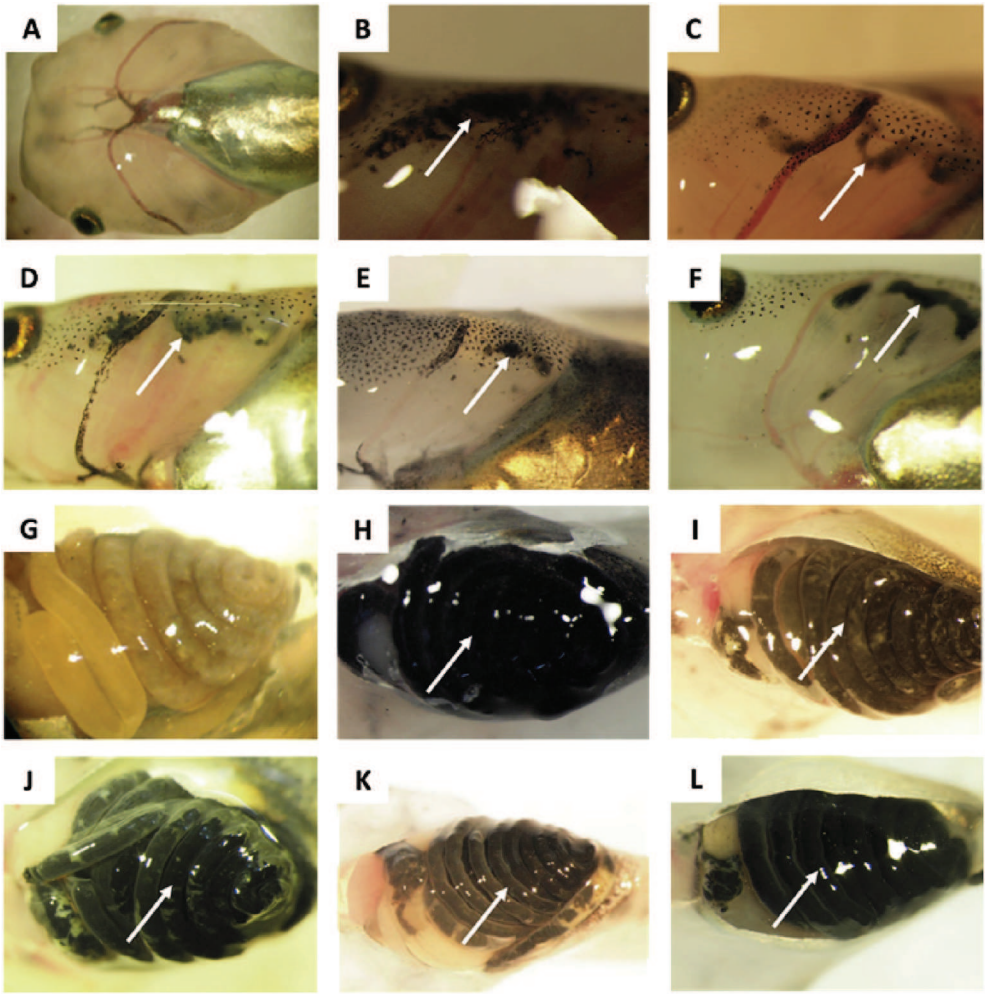

Fig. 3. Macro-observations under binocular of *X. laevis* larvae exposed during 12 days to 10 mg L^{-1} of (C, I) DW-SRNOM and (F, L) GO-B, and 50 mg L^{-1} of (B, H) MW-CMC, (D, J) DW-ox, (E, K) GO-A compared to (A, G) the NC group. CNP agglomerates (indicated by white arrows) were strongly evidenced in the gills (B, C, D, E and F) and in the intestines (H, I, J, K and L) of larvae exposed to each CNP in contrast to the NC group (A, G). (A colour version of this figure can be viewed online.)

on the surface of the CNPs by complex interaction mechanisms, including electrostatic, hydrophobic, π-π and hydrogen-bond interactions [44]. SRNOM and CMC could so coat the surface of CNPs and act as surfactants to counterbalance van der Waals attractions by inducing electrostatic or steric repulsions: this balance of repulsive and attractive forces leads to a thermodynamically stable dispersion [42]. More generally, the presence of biomacromolecules adsorbed on CNTs was demonstrated to significantly delay their agglomeration rate, which can be attributed to steric repulsion [12]. For example, macro-observations of exposure media show that dispersion of DWCNTs in presence of SRNOM (DW-SRNOM) was more stable in the water column than raw CNTs (Fig. 4 A, B). The same results were observed when MWCNTs were dispersed in the presence of CMC [24]. Despite CNP surface is supposed to be covered by organic compounds in the exposure media [40], the dispersed CNPs still fit with the model using surface area, which shows that the presence of organic matter does not influence larvae growth inhibition (also evidenced with the corresponding control experiments).

Another type of chemical dispersion is finally obtained by functionalizing CNPs, leading to the change of their surface chemistry. Thus, hydrophobic raw CNPs could be transformed by various chemical processes in order to form more hydrophilic functions linked by covalent bonds to the surface of the CNPs. In the case of DW-ox [45], GO-A and GO-B (unpublished data), these functional groups are oxygen-based (epoxide, hydroxyl, carboxyl). Hydrophilization of CNTs through oxidation was proved both to prevent them from agglomeration and to enhance their dispersion stability in aqueous media [15]. Similarly, colloidal stability provided by carboxyl groups on the periphery of graphene oxide was reported by Park et al. [46], while basal surfaces of GO include both polar hydroxyl, epoxide groups, and unmodified hydrophobic graphenic domains which can make it acting like a surfactant [47]. According to visual observations, suspensions of oxidized CNPs such as GO-B (Fig. 4 C), GO-A and DW-ox (data not shown) clearly appears more homogeneous in water compared to raw ones. This increased stability could also be explained by a stronger interaction with different components of the media originating from RW (nutrient salts) or food (trace elements, hydrophilic vitamins and other organic compounds). For example, raw CNTs with very few oxygen-containing functional groups were demonstrated to have relatively low sorption capabilities for metal ions [48], whereas their oxidized counterparts exhibit generally higher ones because of their negative charges on which cations can complex with [15,49].

Surfaces coated with organic matter or oxidized surfaces significantly modify physical adsorption and catalytic capabilities of nanomaterials. This is particularly important in regard to

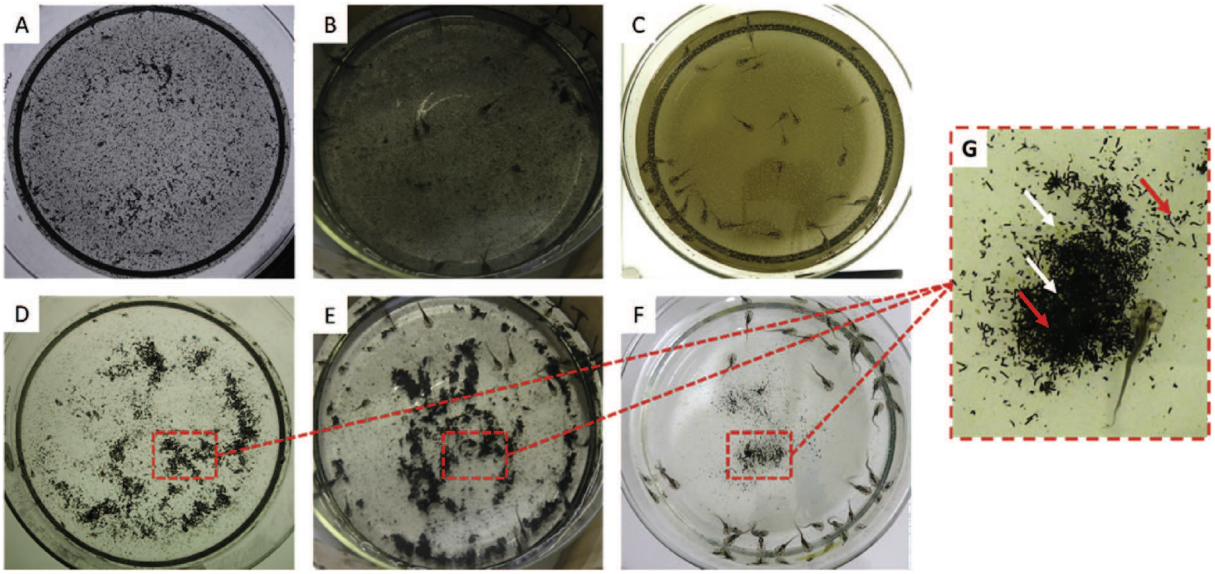

Fig. 4. Visual aspect of the medium of exposure of *X. laevis* larvae exposed to 10 mg L^{-1} of raw MWCNTs (A, D), DW-SRNOM (B, E), and GO-B (C, F). Each CNP exhibits a different state of dispersion more or less homogeneous immediately after renewal (A, B, C) depending on the addition of a chemical dispersant or its oxidation state. Raw MWCNTs appear to be the most heterogeneous as highlighted by the presence of agglomerates (A). For each CNP, the state of dispersion is different between T0h (just after contamination; A, B, C) and T24h (24 h after contamination; D, E, F). In spite of different initial states of dispersion depending on the type of CNPs, the final aspect is rather similar after sedimentation, where a mixture of feces, CNPs (white arrows) and food (red arrows) can be observed (G). (A colour version of this figure can be viewed online.)

biological response [14]. Moreover, depending on the state of dispersion of each CNP (Fig. 4 A, B, and C), their bioavailability for *Xenopus laevis* is modified. As they are pelagic, larvae were more exposed to dispersed CNPs in the water column than raw CNPs. Nevertheless, expressed as a function of CNP surface area, the measured growth endpoint shows no difference between larvae exposed to dispersed and undispersed CNPs. Only CNP surface area appears to describe the observed effects (Fig. 2).

X. laevis larvae are able to feed by both filtration and grazing [50]. This particularity makes it indifferent to the dispersion state of CNPs since it will be exposed by both ways. So, whatever the kind of CNPs and their state of dispersion, they are transferred *via* the general cavity to basket gills and the digestive tract of larvae (Fig. 3) and finally excreted (Fig. 5. B) [37]. In our exposure conditions, *Xenopus* larvae ingest their feces and suspended matter continuously over the 24 h of the medium renewal, leading to a kind of sediment composed of a mixture of agglomerated CNPs and organic matter in the crystallizing dishes. Consequently, whatever the initial state of dispersion and the type of CNPs, the observations of the exposure media after 24 h are rather similar (Fig. 4 D, E, F, and G).

4.3. Biological hypothesis

As filter-feeder organisms, *Xenopus* larvae actively filter the water column containing particles in suspension and ions from RW and food which will be found in basket gills, oral, pharyngeal cavity and intestinal tract. Thus, it appears that regardless of their oxidation state or their load of organic matter, but depending on their surface area, CNPs could lead to larvae growth inhibition.

Growth inhibition (Table 3; Fig. 2) could be explained by several non-exclusive hypotheses. Firstly, as shown in Fig. 3, CNP agglomerates were largely observed in the intestinal tract, with no significant difference whatever the CNPs and the mode of dispersion used. An interaction between nutrients and CNPs could be responsible for a decrease in nutrients absorption all along the digestive tract. Indeed, it has been demonstrated that the hydrophobic surfaces of CNPs could adsorb solutes with a molecular structure presenting hydrophobicity, planarity/sp^2 hybridization for π-π interactions, and positive charge (which is opposite to that of most of carbon surfaces) [51]. CNP adsorption capacity was exhibited to increase with a larger surface area [15]. In addition, CNPs shown no significant change in their physico-chemical properties towards physiological acidic conditions as described for the human digestive tract [52], whom gastric fluid is more acid (pH = 2.9) [53] than *Xenopus* tadpole one (pH = 7.8) [54]. The presence of CNPs in the digestive tract could thus lead to a sequestration of essential micronutrients such as amino-acids, vitamins [51], but also nucleic acids and other hydrophobic macromolecules [14]. These associations may reduce the nutrient intake and their bioavailability in the larvae. In addition, it should be noticed that CNPs are assumed not to pass through the intestinal barrier, as previously assessed for CNTs in *Xenopus* [19] and similarly shown for MWCNTs in *Daphnia* [17], GO derivatives in the mouse [55] and bare fluorescent NDs in worms [56]. This could be explained because CNPs form aggregates inside the intestinal lumen (Fig. 3 H-L) that are too large to enter the cells. In addition, CNPs may not be recognized and taken up by the active transport system of the intestinal cells. However, although experimental data is missing, the molecular dynamics simulations proposed by Titov et al. [57] suggest that GRMs could form stable hybrids with biological lipid bilayers (where they would be passively localized in the hydrophobic core). It could be hypothesized that such a configuration with the intestinal cell could form a potential, partial, physical barrier limiting nutrients intake of the larvae. Finally, the presence of CNPs in the digestive tract could lead to a partial starvation in *Xenopus*, increasing with their surface area. Starvation is the main reason that could explain the observed growth inhibition in *Xenopus laevis* [58], and such an effect could be a consequence of metabolic priorities as suggested by Sumpter et al. [59] and Guderley et al. [60] in the fish.

Secondly, Fig. 3 reveals the macro-presence of CNP agglomerates inside the gills. Like intestine, gills represent a large surface of exchange, so it also appears more logical to consider the surface of CNPs rather than their mass concerning their interaction with gills. In *Xenopus laevis* larvae, gills are well vascularized for gas exchange but they also have a function of food entrapment [61]. Our

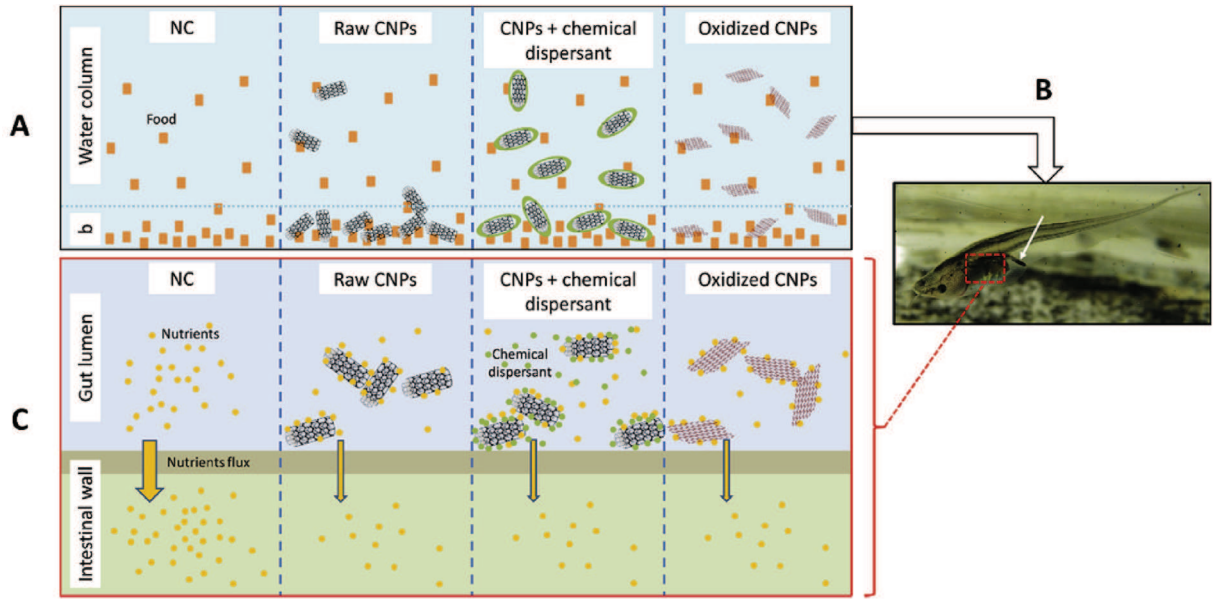

Fig. 5. Theoretical representation of growth inhibition mechanisms of *X. laevis* larvae by ingestion of carbon based nanoparticles (CNPs). 5.A: different modes of exposure of *X. laevis* larvae to a given dose of CNPs compared to the negative control (NC) group; b: bottom of the container. 5.B: photography of a *Xenopus* larva in the water column exposed to CNPs. Whatever the state of dispersion and the type of CNPs, these latest are excreted as represented by the white arrow. 5.C: theoretical representation of the decrease of absorption of nutrients in the intestine (as shown by the thickness of the orange arrows). In spite of different states of dispersion depending on the CNP type, ingested CNPs limit the absorption of nutrients in the same way, depending on their surface area (5.C). (A colour version of this figure can be viewed online.)

observations suggest a gill injury which could be at the origin of both decreased efficiency of food intake and a respiratory disturbance. In presence of MWCNTs, modifications in gaseous exchanges were evidenced [62]. Smith et al. [63] reported similar results in rainbow trout exposed to single-walled CNTs with a dose-dependent increase in ventilation rate. Eventual gill clogging may also force *Xenopus* larvae to move to the surface to breath thanks to their lungs [61]. This aerial breathing represents an energetic cost which could finally affect the larval growth. A possible disruption of cutaneous respiration by CNPs coating the skin could be possible and should not be underestimated since skin accounts for the predominant route of O_2 uptake in air-breathing tadpoles [64].

Finally, an important mechanism underlying CNP toxicity is the induction of oxidative stress because of direct or indirect generation of reactive oxygen species (ROS) [14]. Oxidative stress could be the results of many processes including starvation [65] and gills clogging at the origin of the modification of the red-ox status of gills cells [66]. Among critical determinants that can affect ROS generation, Fu et al. [13] identified that nanoparticles with higher specific surface areas could lead to an increased production of ROS compared to their bulk-size counterparts. This induction of ROS has been observed in many organisms and tissues exposed to different allotropic forms of carbon [66–68]. In living organisms, cellular homeostasis involves a balance between ROS generation and ROS elimination by antioxidant enzymes such as catalase, superoxide dismutase, or glutathione peroxidase. Induction of defense systems against oxidative stress could represent an energetic cost leading to a lower amount of energy available for *Xenopus* larvae growth.

5. Conclusion

The toxicity of different types of CNPs on *Xenopus laevis* larvae growth rate was expressed as a function of two dose metrics: mass or surface concentration. The statistical comparison between the two models clearly shows that CNP surface area is the most relevant metric that could describe the effect of CNPs on larvae growth. Growth appears similarly impacted whatever the allotropic form of CNPs or their dispersion state, including covalent (oxidized CNPs) and non-covalent dispersions (raw CNPs added with a chemical dispersant). This suggests that growth inhibition mechanisms are mostly dependent on the specific surface area of each CNP. Such growth inhibition could be explained by the trophic behavior of larvae, which are both filter-feeder and grazer: they could entrap CNPs both in water column when there are dispersed, or at the bottom if they have settled down. Once ingested, CNPs are assumed to adsorb nutrients (proportionally to their surface area) and not to pass through the intestinal barrier, leading to a decrease in nutrients absorption required for growth. A minor point is that CNPs could be responsible for respiratory disturbance by clogging the gills, forcing larvae to compensate by aerial breathing which represents an energetic cost.

In agreement with our previous work [11] related to raw CNPs only, this conclusion could so extend to a larger range of CNPs, including more environmentally realistic conditions of dispersion. Thus, specific surface area of most of the carbon-based nanoparticles likely to be found in the environment such as carbon nanotubes, few layer graphene, graphene oxide and nanodiamonds could thus be used for risk assessment by predicting their potential effect on the environment. More work is currently in progress with other nanocarbon species, such as for example reduced graphene oxide, aiming at extending this conclusion to “nanocarbons” in general.

Although literature generally reports higher toxicity for the dispersed CNPs, this is not the case in our study. However, only chronic toxicity dealing with growth inhibition was investigated in this work. No mortality was observed either, but other endpoints like genotoxicity would deserve further attention. In addition, our conclusion requires to be emphasized by new similar studies before being generalized to all CNPs. The same applies for other engineered nanoparticles (like metals and oxides) which would benefit from deeper analysis to know if they follow the same pattern or not. Furthermore, our model organism *X. laevis* is representative of anuran amphibian species at larval stage, whereas organisms with other feeding behavior would probably not have suffered from the

same growth inhibition. Other organisms should thereby be tested to know if this conclusion is proper to grazer, filter-feeders or can be generalized to a larger extent.

Declaration of interest

The authors report no conflict of interest. The authors alone are responsible for the content and writing of the paper.

Acknowledgements

This research was supported by the French Ministry of National Education, Higher Education and Research. The research has also received funding from the European Union Seventh Framework Programme under grant agreement n°604391 Graphene flagship.

Thanks to L. Verneuil for his preparation of DW-SRNOM for the transmission electron microscopy.

References

[1] M.S. Mauter, M. Elimelech, Environmental applications of carbon-based nanomaterials, Environ. Sci. Technol. 42 (16) (2008) 5843–5859.
[2] Q. Wang, B. Arash, A review on applications of carbon nanotubes and graphenes as nano-resonator sensors, Comput. Mater. Sci. 82 (2014) 350–360.
[3] B. Zhang, Y. Wang, G. Zhai, Biomedical applications of the graphene-based materials, Mater. Sci. Eng. C 61 (2016) 953–964.
[4] C. Zhu, D. Du, Y. Lin, Graphene-like 2D nanomaterial-based biointerfaces for biosensing applications, Biosens. Bioelectron. 89 (2017) 43–55.
[5] M. Zhou, Z. Wang, X. Wang, Carbon Nanotubes for Sensing Applications, Elsevier Inc., 2017.
[6] D. Gon Lim, R. Ena Prim, K. Hyun Kim, E. Kang, K. Park, S. Hoon Jeong, Combinatorial nanodiamond in pharmaceutical and biomedical applications, Int. J. Pharm. 514 (2016) 41–51.
[7] G. Oberdörster, E. Oberdörster, J. Oberdörster, Nanotoxicology: an emerging discipline evolving from studies of ultrafine particles, Environ. Health Perspect. 113 (7) (2005) 823–839.
[8] M. Auffan, J. Rose, J.-Y. Bottero, G.V. Lowry, J.-P. Jolivet, M.R. Wiesner, Towards a definition of inorganic nanoparticles from an environmental, health and safety perspective, Nat. Nanotechnol. 4 (10) (2009) 634–641.
[9] M. Hull, A.J. Kennedy, C. Detzel, P. Vikesland, M.A. Chappell, Moving beyond mass: the unmet need to consider dose metrics in environmental nanotoxicology studies, Environ. Sci. Technol. 46 (2012) 10881–10882.
[10] T. Stoeger, C. Reinhard, S. Takenaka, A. Schroeppel, E. Karg, B. Ritter, et al., Instillation of six different ultrafine carbon particles indicates a surface area threshold dose for acute lung inflammation in mice, Environ. Health Perspect. 114 (3) (2006) 328–333.
[11] A. Mottier, F. Mouchet, C. Laplanche, S. Cadarsi, L. Lagier, J.-C. Arnault, et al., Surface area of carbon nanoparticles: a dose metric for a more realistic ecotoxicological assessment, Nano Lett. 16 (2016) 3514–3518.
[12] N.B. Saleh, L.D. Pfefferle, M. Elimelech, Influence of biomacromolecules and humic acid on the aggregation kinetics of single-walled carbon nanotubes, Environ. Sci. Technol. 44 (7) (2010) 2412–2418.
[13] P.P. Fu, Q. Xia, H. Hwang, P.C. Ray, H. Yu, Mechanisms of nanotoxicity: generation of reactive oxygen species, J. Food Drug Anal. 22 (2014) 64–75.
[14] V.C. Sanchez, A. Jachak, R.H. Hurt, A.B. Kane, Biological interactions of graphene-family nanomaterials : an interdisciplinary review, Chem. Res. Toxicol. 25 (2012) 15–34.
[15] S. Boncel, J. Kyzioł-Komosińska, I. Krzyżewska, J. Czupioł, Interactions of carbon nanotubes with aqueous/aquatic media containing organic/inorganic contaminants and selected organisms of aquatic ecosystems – a review, Chemosphere 136 (2015) 211–221.
[16] E.J. Petersen, R.A. Pinto, D.J. Mai, P.F. Landrum, W.J. Weber Jr., Influence of polyethyleneimine graftings of multi-walled carbon nanotubes on their accumulation and elimination by and toxicity to Daphnia magna, Environ. Sci. Technol. 45 (3) (2011) 1133–1138.
[17] A.J. Edgington, A.P. Roberts, L.M. Taylor, M.M. Alloy, J. Reppert, A.M. Rao, et al., The influence of natural organic matter on the toxicity of multiwalled carbon nanotubes, Environ. Toxicol. Chem. 29 (11) (2010) 2511–2518.
[18] D. Li, D.Y. Lyon, Q. Li, P.J.J. Alvarez, Effect of soil sorption and aquatic natural organic matter on the antibacterial activity of a fullerene water suspension, Environ. Toxicol. Chem. 27 (9) (2008) 1888–1894.
[19] F. Mouchet, P. Landois, P. Puech, E. Pinelli, E. Flahaut, L. Gauthier, Carbon nanotube ecotoxicity in amphibians: assessment of multiwalled carbon nanotubes and comparison with double-walled carbon nanotubes, Nanomed. Nanotechnol. Biol. Med. 5 (6) (2010) 963–974.
[20] F. Mouchet, P. Landois, E. Sarremejean, G. Bernard, P. Puech, E. Pinelli, et al., Characterisation and in vivo ecotoxicity evaluation of double-wall carbon nanotubes in larvae of the amphibian Xenopus laevis, Aquat. Toxicol. 87 (2008) 127–137.
[21] L. Gauthier, "The amphibian micronucleus test, a model for in vivo monitoring of genotoxic aquatic pollution," *Alytes*, Int. J. Batrachol. 14 (2) (1996) 53–84.
[22] L. Gauthier, E. Tardy, F. Mouchet, J. Marty, Biomonitoring of the genotoxic potential (micronucleus assay) and detoxifying activity (EROD induction) in the River Dadou (France), using the amphibian Xenopus laevis, Sci. Total Environ. 323 (2004) 47–61.
[23] E. Flahaut, R. Bacsa, A. Peigney, C. Laurent, Gram-scale CCVD synthesis of double-walled carbon nanotubes, Chem. Commun. R. Soc. Chem. (2003) 1442–1443.
[24] F. Bourdiol, F. Mouchet, A. Perrault, I. Fourquaux, L. Datas, C. Gancet, et al., Biocompatible polymer-assisted dispersion of multi walled carbon nanotubes in water, application to the investigation of their ecotoxicity using Xenopus laevis amphibian larvae, Carbon N. Y. 54 (2013) 175–191.
[25] W.S. Hummers, R.E. Offeman, Preparation of graphitic oxide, J. Am Chem. Soc 80 (6) (1958) 1339.
[26] B. Lobato, C. Merino, V. Barranco, T.A. Centeno, Large-scale conversion of helical-ribbon carbon nanofibers to a variety of graphene-related materials, RSC Adv. 6 (2016) 57514–57520.
[27] L. Tabet, C. Bussy, N. Amara, A. Setyan, A. Grodet, M.J. Rossi, et al., Adverse effects of industrial multiwalled carbon nanotubes on human pulmonary cells, J. Toxicol. Environ. Health. A 72 (2009) 60–73.
[28] Agence nationale de sécurité sanitaire de l'alimentation de l'environnement et du travail (Anses), Avis relatif à « l'évaluation des risques liés au GRAPHISTRENGTH C100 réalisée dans le cadre du programme Genesis »; Saisine n° 2007-SA-0417, 2011.
[29] V. Leon, A.M. Rodriguez, P. Prieto, M. Prato, E. Vazquez, Exfoliation of graphite with triazine derivatives under ball-milling conditions: preparation of few-layer graphene via selective noncovalent interactions, ACS Nano 8 (1) (2014) 563–571.
[30] L. Verneuil, J. Silvestre, F. Mouchet, E. Flahaut, J.-C. Boutonnet, F. Bourdiol, et al., Multi-walled carbon nanotubes, natural organic matter, and the benthic diatom Nitzschia palea: "A sticky story", Nanotoxicology 9 (2) (2015) 219–229.
[31] L. Verneuil, Toxicité environnementale et écotoxicité de nanotubes de carbone chez des diatomées benthiques : de la cellule au biofilm, Université Paul Sabatier, France, 2015. PhD thesis.
[32] P.D. Nieuwkoop, J. Faber, Normal Tables of Xenopus laevis (Daudin), North-Holland, Amsterdam, 1956.
[33] ISO/FDIS 21427-1. Water Quality-evaluation of Genotoxicity by Measurement of the Induction of Micronuclei-part 1: Evaluation of Genotoxicity Using Amphibian Larvae, International Organization for Standardization, Geneva, 2006.
[34] A.D.R. McQuarrie, C.-L. Tsai, Regression and Time Series Model Selection, World Scie, World Scientific Publishing Co. Re. Ltd, 1998. P 0 Box 128, Farrer Road, Singapore 912805 USA ofjice: Suite lB, 1060 Main Street, River Edge, NJ 07661 UK ofice: 57 Shelton Street, Covent Garden, London WC2H 9HE Regression.
[35] K.P. Burnham, D.R. Anderson, Model Selection and Multimodel Inference: a Practical Information-theoretic Approach, 2002. Second edi.
[36] R. Core Team, R: a Language and Environment for Statistical Computing, R Foundation for Statistical Computing, Vienna, Austria, 2016.
[37] L. Muzi, F. Mouchet, S. Cadarsi, I. Janowska, J. Russier, C. Ménard-Moyon, et al., Examining the impact of multi-layer graphene using cellular and amphibian models, 2D Mater. 3 (2) (2016) 1–10.
[38] J. Cheng, C. Man Chan, L.M. Veca, W. Lin Poon, P. Kwok Chan, L. Qu, et al., Acute and long-term effects after single loading of functionalized multi-walled carbon nanotubes into zebrafish (Danio rerio), Toxicol. Appl. Pharmacol. 235 (2009) 216–225.
[39] E. Heister, C. Lamprecht, V. Neves, C. Tîlmaciu, L. Datas, E. Flahaut, et al., Higher dispersion efficacy of functionalized carbon nanotubes in chemical and biological environments, ACS Nano 4 (5) (2010) 2615–2626.
[40] R. Grillo, A.H. Rosa, L.F. Fraceto, Engineered nanoparticles and organic matter: a review of the state-of-the-art, Chemosphere 119 (2015) 608–619.
[41] B. Smith, K. Wepasnick, K.E. Schrote, H. Cho, W.P. Ball, D.H. Fairbrother, Influence of surface oxides on the colloidal stability of multi-walled carbon nanotubes: a structure-property relationship, Langmuir Artic. 25 (17) (2009) 9767–9776.
[42] J. Hilding, E.A. Grulke, Z. George Zhang, F. Lockwood, Dispersion of carbon nanotubes in liquids, J. Dispers. Sci. Technol. 24 (1) (2003) 1–41.
[43] J. Gigault, B. Grassl, G. Lespes, Size characterization of the associations between carbon nanotubes and humic acids in aqueous media by asymmetrical flow field-flow fractionation combined with multi-angle light scattering, Chemosphere 86 (2012) 177–182.
[44] K. Yang, B. Xing, Adsorption of fulvic acid by carbon nanotubes from water, Environ. Pollut. 157 (2009) 1095–1100.
[45] T. Bortolamiol, P. Lukanov, A. Galibert, B. Soula, P. Lonchambon, L. Datas, et al., Double-walled carbon nanotubes : quantitative purification assessment, balance between purification and degradation and solution filling as an evidence of opening, Carbon N. Y. 78 (2014) 79–90.
[46] S. Park, J. An, I. Jung, R.D. Piner, S. Jin An, X. Li, et al., Colloidal suspensions of highly reduced graphene oxide in a wide variety of organic solvents, Nano Lett. 9 (4) (2009) 1593–1597.
[47] L.J. Cote, J. Kim, V.C. Tung, J. Luo, F. Kim, J. Huang, Graphene oxide as surfactant sheets, Pure Appl. Chem. 83 (1) (2011) 95–110.
[48] X. Tian, T. Li, K. Yang, Y. Xu, H. Lu, D. Lin, Effect of humic acids on the

physicochemical property and Cd(II) sorption of multiwalled carbon nanotubes, Chemosphere 89 (2012) 1316–1322.
[49] H.-H. Cho, K. Wepasnick, B.A. Smith, F.K. Bangash, D.H. Fairbrother, W.P. Ball, Sorption of aqueous Zn[II] and Cd[II] by multiwall carbon nanotubes: the relative roles of oxygen-containing functional groups and graphenic carbon, Langmuir 26 (2) (2010) 967–981.
[50] D.B. Seale, K. Hoff, R. Wassersug, Xenopus laevis larvae (Amphibia, Anura) as model suspension feeders, Hydrobiologia 87 (1982) 161–169.
[51] L. Guo, A. Von Dem Bussche, M. Buechner, A. Yan, A.B. Kane, R.H. Hurt, Adsorption of essential micronutrients by carbon nanotubes and the implications for nanotoxicity testing, Small 4 (6) (2008) 721–727.
[52] M. Kucki, P. Rupper, C. Sarrieu, M. Melucci, E. Treossi, A. Schwarz, et al., Interaction of graphene-related materials with human intestinal cells: an in vitro approach, Nanoscale 8 (2016) 8749–8760.
[53] D.E. Beasley, A.M. Koltz, J.E. Lambert, N. Fierer, R.R. Dunn, The evolution of stomach acidity and its relevance to the human microbiome, PLoS One 10 (7) (2015) 1–12.
[54] I. Griffiths, The form and function of the fore-gut in anuran larvae (amphibia, salientia) with particular reference to the manicotto glandulare, J. Zool. 137 (2) (1961) 249–283.
[55] K. Yang, H. Gong, X. Shi, J. Wan, Y. Zhang, Z. Liu, In vivo biodistribution and toxicology of functionalized nano-graphene oxide in mice after oral and intraperitoneal administration, Biomaterials 34 (2013) 2787–2795.
[56] N. Mohan, C. Chen, H. Hsieh, Y. Wu, H. Chang, In vivo imaging and toxicity assessments of fluorescent nanodiamonds in Caenorhabditis elegans, Nano Lett. 10 (2010) 3692–3699.
[57] A. V Titov, P. Kral, R. Pearson, Sandwiched graphene-membrane superstructures, ACS Nano 4 (1) (2010) 229–234.
[58] G. Hilken, J. Dimigen, F. Iglauer, Growth of Xenopus laevis under different laboratory rearing conditions, Lab. Anim. 29 (2) (1995) 152–162.
[59] J.P. Sumpter, P.Y. Le Bail, A.D. Pickering, T.G. Pottinger, J.F. Carragher, The effect of starvation on growth and plasma growth hormone concentrations of rainbow trout, Oncorhynchus mykiss, Gen. Comp. Endocrinol. 83 (1991) 94–102.
[60] H. Guderley, D. Lapointe, M. Bédard, J.-D. Dutil, Metabolic priorities during starvation: enzyme sparing in liver and white muscle of Atlantic cod, Gadus morhua L, Comp. Biochem. Physiol. Part A 135 (2) (2003) 347–356.
[61] M.E. Feder, R.J. Wassersug, Aerial versus aquatic oxygen consumption in larvae of the clawed frog, Xenopus laevis, J. Exp. Biol. 108 (1984) 231–245.
[62] R. Saria, Etude des mécanismes de toxicité des nanotubes de carbone multiparois chez le modèle amphibien Xenopus laevis, Université Paul Sabatier, France, 2014. PhD Thesis.
[63] C.J. Smith, B.J. Shaw, R.D. Handy, Toxicity of single walled carbon nanotubes to rainbow trout, (Oncorhynchus mykiss): respiratory toxicity, organ pathologies, and other physiological effects, Aquat. Toxicol. 82 (2007) 94–109.
[64] W.W. Burggren, M.E. Feder, A.W. Pinder, Temperature and the balance between aerial and aquatic respiration in larvae of Rana berlandieri and Rana catesbeiana, Physiol. Zool. 56 (2) (1983) 263–273.
[65] A.E. Morales, A. Pérez-Jiménez, M.C. Hidalgo, E. Abellan, G. Cardenete, Oxidative stress and antioxidant defenses after prolonged starvation in Dentex dentex liver, Comp. Biochem. Physiol. Part C 139 (2004) 153–161.
[66] R. Saria, F. Mouchet, A. Perrault, E. Flahaut, C. Laplanche, J. Boutonnet, et al., Short term exposure to multi-walled carbon nanotubes induce oxidative stress and DNA damage in Xenopus laevis tadpoles, Ecotoxicol. Environ. Saf. 107 (2014) 22–29.
[67] P. Jackson, N.R. Jacobsen, A. Baun, R. Birkedal, D. Kühnel, K. Alstrup Jensen, et al., Bioaccumulation and ecotoxicity of carbon nanotubes, Chem. Cent. J. 7 (1) (2013) 154–165.
[68] M. Chen, J. Yin, Y. Liang, S. Yuan, F. Wang, M. Song, et al., Oxidative stress and immunotoxicity induced by graphene oxide in zebrafish, Aquat. Toxicol. 174 (2016) 54–60.